

## Surface optical vortices

V. E. Lembessis,<sup>1,\*</sup> M. Babiker,<sup>1</sup> and D. L. Andrews<sup>2</sup>

<sup>1</sup>*Department of Physics, University of York, Heslington, York YO10 5DD, United Kingdom*

<sup>2</sup>*School of Chemical Sciences, University of East Anglia, Norwich NR4 7TJ, United Kingdom*

(Received 18 September 2008; published 14 January 2009)

It is shown how the total internal reflection of orbital-angular-momentum-endowed light can lead to the generation of evanescent light possessing rotational properties in which the intensity distribution is firmly localized in the vicinity of the surface. The characteristics of these *surface optical vortices* depend on the form of the incident light and on the dielectric mismatch of the two media. The interference of surface optical vortices is shown to give rise to interesting phenomena, including pattern rotation akin to a surface optical Ferris wheel. Applications are envisaged to be in atom lithography, optical surface tweezers, and spanners.

DOI: 10.1103/PhysRevA.79.011806

PACS number(s): 42.50.Tx, 37.10.De

Recent years have witnessed the emergence of a branch of optics concerned with the production and applications of twisted light. This is a class of laser light distinguished by an azimuthal phase dependence  $\exp(il\phi)$ , where  $l$  is an integer and  $\phi$  is the azimuthal angle about the beam axis in cylindrical coordinates. Such light was shown in a pioneering paper by Allen *et al.* [1] to possess an orbital angular momentum  $l\hbar$ , distinct from the spin angular momentum associated with wave polarization. The prototypical set of twisted light beams are the well-defined Laguerre-Gaussian beams, which can now readily be created in the laboratory. Laguerre-Gaussian laser light has been investigated over the last two decades or so, and its effects on matter, both in the bulk and as single atoms, have been considered. It is now well established that twisted light can be used as an optical device capable of rotating small objects [2–5], supplementing the capacity it shares with any laser light to influence translational motion (optical tweezers). The effects of light on single atoms and molecules have been explored theoretically, identifying cooling and heating effects of translational, as well as the rotational, motion when atoms are subject to twisted light. The rotational motion of the atoms has been shown to arise from a laser-induced torque [6] associated with the azimuthal component of the light pressure force. It has also been established that the transfer of orbital angular momentum to dipole-active atoms and molecules involves only the center-of-mass motion, rather than the internal dynamics [7]. Multiple Laguerre-Gaussian beams have been shown to provide different optical molasses situations in two and three dimensions [8–10].

The interference of different Laguerre-Gaussian light beams has recently been studied experimentally, revealing a rich variety of intensity distributions. For copropagating beams of equal and opposite values of  $l$ , but with slightly differing frequencies, it has been shown experimentally that the interference pattern forms a so-called optical Ferris wheel in that the pattern rotates at an angular frequency that depends on  $l$  and the frequency separation of the two beams [11]. The authors of this article point out that the light inten-

sity distribution may be used to trap atoms, but the copropagation of the two beams is disadvantageous in that there are no optical molasses forces that work to cool the atoms axially, as in the case of counterpropagating beams.

A different interference scenario is one involving the internal reflection of twisted light at a planar surface between an optically dense medium, within which the light is incident, and a vacuum. As far as we know, this simple and easily realizable experimental situation has not been considered before in the context of surface-atom manipulation using Laguerre-Gaussian light. Nevertheless, evanescent light due to conventional beams has been successfully used in atomic mirrors [12] and its use in surface manipulation has been considered for small objects at surfaces [13–17], rather than near-resonance atoms and molecules. As we show here for Laguerre-Gaussian beams, the evanescent light that emerges in the vacuum region is exponentially decaying with the distance normal to the surface, but carries the in-plane distribution of the incident beam and its angular momentum properties. Superimposed on this is a plane wave traveling along the surface with a wave vector equal to the component of the axial wave vector of the incident beam. The field distribution thus created forms a surface optical vortex, with a well-defined orbital angular momentum. Counterpropagating or copropagating evanescent surface optical vortices can, in principle, also be created. Clearly, there is ample scope for interference effects, different possibilities for atom trapping and atom manipulation at a surface, and optical surface spanners and tweezers. In what follows we outline the physics underlying surface optical vortices and detail their possible involvement in the applications mentioned above.

Consider first the electric field of a Laguerre-Gaussian (LG) beam traveling along  $z$  in a medium of a constant refractive index  $n$ , characterized by the integers  $l$  and  $p$ , circular frequency  $\omega$ , and axial wave vector  $k = nk_0$ , where  $k_0 = \omega/c$  is the wave vector in vacuum. For LG light plane polarized along  $\hat{y}$ , the field vector can be written in cylindrical coordinates as

$$\mathbf{E}_{klp}^I(r, \phi, z) = \hat{y} \mathcal{F}_{klp}(r, z) e^{i(kz - \omega t)} e^{il\phi}, \quad (1)$$

where  $\mathcal{F}_{klp}(r, z)$  is the standard envelope function of  $r$  and  $z$ , with  $r = \sqrt{x^2 + y^2}$ :

\*On leave of absence from New York College of Athens, 38 Amalias Avenue, GR 105 58, Athens, Greece.

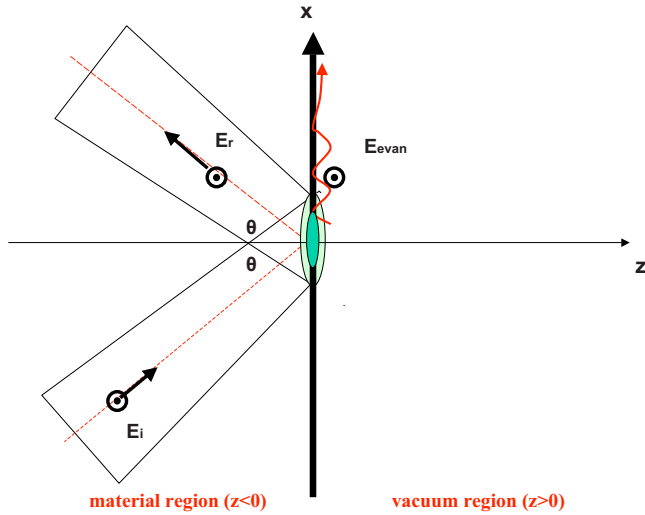


FIG. 1. (Color online) Laguerre-Gaussian light internally reflected at an angle  $\theta$  greater than the critical angle (schematic). The incident beam is arranged such that at  $\theta=0$  the beam waist coincides with the surface at  $z=0$ . The evanescent light possesses angular momentum properties, but is confined near the surface, exponentially decaying in the direction normal to the surface.

$$\mathcal{F}_{klp}(r, z) = \mathcal{E}_{k00} \frac{C_{lp}}{(1 + z^2/z_R^2)^{1/2}} \left( \frac{\sqrt{2}r}{w(z)} \right)^{|l|} \times L_p^{|l|} \left( \frac{2r^2}{w^2(z)} \right) e^{-r^2/w^2(z)} e^{i\Theta_{GR}(z)}. \quad (2)$$

Here  $\mathcal{E}_{k00}$  is the amplitude for a corresponding plane wave of wave vector  $k$ ,  $C_{lp}$  is a mode constant, and the beam waist at axial coordinate  $z$  is  $w(z)$  such that  $w^2(z) = 2(z^2 + z_R^2)/kz_R$ , where  $z_R$  is the Rayleigh range. The last phase factor in Eq. (2) accommodates both the Guoy phase and the change in beam curvature with axial position. We have

$$\Theta_{GR}(z) = \frac{kr^2z}{2(z^2 + z_R^2)} + (2p + |l| + 1)\tan^{-1}(z/z_R). \quad (3)$$

Note that the plane  $z=0$  corresponds to the minimum beam waist  $w(0)=w_0$  and on this plane the Guoy and curvature terms in Eq. (3) both vanish.

Such a light field can be arranged, as shown in Fig. 1, to strike the internal planar surface of a medium, in which it is propagating—that is, in contact with the vacuum. If the interface with the vacuum occupies the plane  $z=0$  and the angle of incidence,  $\theta$ , exceeds the total internal reflection angle, an evanescent mode is created in the vacuum. The main requirements are the applicability of the standard phase-matching condition of boundary reflection and the condition that the electric field vector component tangential to the surface be continuous across the boundary. To be able to define the evanescent electric field, we must first obtain expressions appropriate for a beam incident at an angle  $\theta$ . This is obtainable by simple rotational transformations of the expressions in Eqs. (1)–(3).

The fields of a Laguerre-Gaussian beam propagating in a general direction can be constructed from the formalism out-

lined above by the application of two coordinate transformations, the first transformation rotating the beam as a rigid body about the  $y$  axis by angle  $\alpha$  and the second rotates the resultant beam in the  $z$  plane about the  $x$  axis by an angle  $\beta$ . The compound transformation produces the relations

$$x \rightarrow x' = x \cos \alpha + z \sin \alpha, \quad (4)$$

$$y \rightarrow y' = -x \sin \alpha \sin \beta + y \cos \beta + z \cos \alpha \sin \beta, \quad (5)$$

$$z \rightarrow z' = -x \sin \alpha \cos \beta - y \sin \beta + z \cos \alpha \cos \beta. \quad (6)$$

Equations (4)–(6) are useful in general situations involving multiple beams of different orientations incident on the surface. For a single beam the expressions simplify considerably. To determine the field distributions of the incident beam, we choose  $\alpha=\theta$  and  $\beta=0$ , and for the internally reflected light, we have  $\alpha=\pi-\theta$  and  $\beta=0$ , as shown in Fig. 1. The continuity of the electric field vector tangential to the surface, along with the exponential decay with the coordinate  $z$ , determines the form of the evanescent field in the vacuum region. We have

$$\mathbf{E}_{klp}^{evan}(x, y, z) = 2\mathbf{E}_{klp}^I(x \rightarrow x \cos \theta; y; z \rightarrow -x \sin \theta) \times e^{-zk_0\sqrt{n^2 \sin^2 \theta - 1}} e^{-ik_0nx \sin \theta}. \quad (7)$$

The explicit form of the evanescent electric field that displays the angular momentum properties, as well as the mode characteristics, is as follows:

$$\begin{aligned} \mathbf{E}_{klp}^{evan}(x, y, z) &= \hat{y} \frac{\mathcal{E}_{000}C_{lp}}{(1 + x^2 \sin^2 \theta/z_R^2)^{1/2}} \left( \frac{\sqrt{2}(x^2 \cos^2 \theta + y^2)}{w_0^2(1 + x^2 \sin^2 \theta/z_R^2)^{1/2}} \right)^{|l|} \\ &\times \exp\left(-\frac{(x^2 \cos^2 \theta + y^2)}{w_0^2(1 + x^2 \sin^2 \theta/z_R^2)^{1/2}}\right) L_p^{|l|} \\ &\times \left( \frac{x^2 \cos^2 \theta + y^2}{w_0^2(1 + x^2 \sin^2 \theta/z_R^2)^{1/2}} \right) \\ &\times \exp\{-zk_0\sqrt{n^2 \sin^2 \theta - 1} - ik_0nx \sin \theta\} \\ &\times \exp[il \arctan(y/x \cos \theta)]. \end{aligned} \quad (8)$$

Note that the above expression for the evanescent light bears the vorticity nature in that it is characterized by the azimuthal phase dependence  $\exp[il \arctan(y/x \cos \theta)]$  of the incident and internally reflected light. The important point to bear in mind in this context is that the field distribution associated with this vortex is concentrated on the surface, rather than axially, as in normal Laguerre-Gaussian light in an unbounded space. The typical exponential decay of the evanescent light intensity along  $z$  (i.e., perpendicular to the interface) is shown in Fig. 2. This is governed by the factor  $\exp[-2zk_0\sqrt{n^2 \sin^2 \theta - 1}]$ , which is independent of the integers  $l$  and  $p$ . The length scale of the exponential decay along  $z$  is seen, from Fig. 2, to span a small fraction of the wavelength, indicating that the evanescent light does not play a significant role in the trapping normal to the surface. Adsorbed atoms are generally subject to the a much more strongly attractive van der Waal potential.

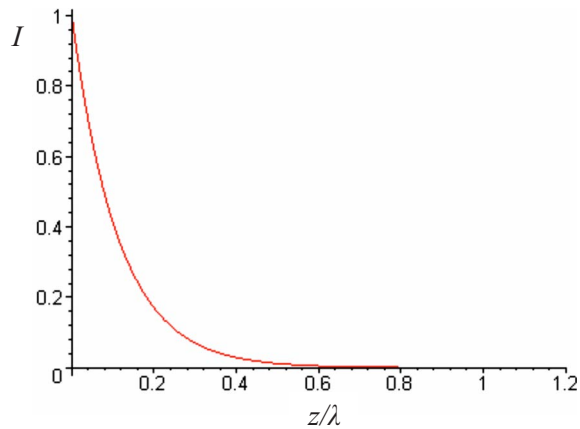


FIG. 2. (Color online) Intensity variations of the evanescent surface optical vortex (arbitrary units) with distance normal to the surface (in units of wavelength  $\lambda$ ). This variation is independent of the values of  $l$  and  $p$ .

The intensity distribution corresponding to the evanescent light created by an incident Laguerre-Gaussian beam for which  $l=1$  and  $p=0$  is shown in Fig. 3, plotted in the  $(x,y)$  plane at  $z=0$ . It is seen that the evanescent light possesses well-defined intensity maxima and minima that can be used to trap adsorbed atoms with transition frequencies appropriately detuned from the frequency  $\omega$  of the light. Note that the profile of the intensity distribution is, in fact, no longer circular, but elliptical, because the light strikes the surface at the angle of incidence  $\theta$ ; the ellipticity increases with increasing  $\theta$ .

The case  $l=3$  and  $p=2$ , with the same parameters as in earlier figures, is shown in Fig. 4. This case presents a more complex field distribution for the corresponding surface optical vortex. Clearly the field distributions for any values of the parameters  $l$  and  $p$  can be obtained in a similar manner: we can in principle create a surface vortex of any order, confirming that the surface optical vortex phenomenon is quite general.

Consider now the case of copropagating incident beams

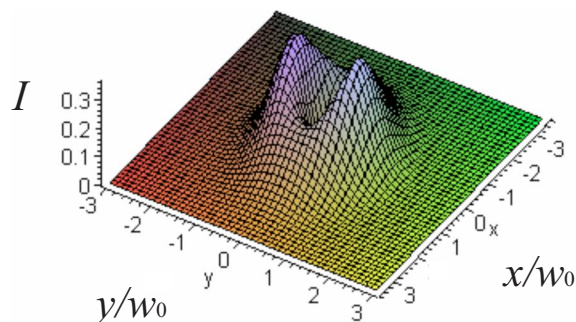


FIG. 3. (Color online) Intensity distribution (arbitrary units) on the surface  $z=0$  for the surface vortex arising from internally reflecting a Laguerre-Gaussian light beam for which  $l=1$  and  $p=0$ . Distances are measured in units of the beam waist  $w_0$ . The light has a wavelength  $\lambda=590$  nm, and beam waist is taken as  $w_0=35\lambda$ , corresponding to a long Rayleigh range  $z_R \approx 2.27 \times 10^{-3}$  m. The refractive index is assumed to be  $n=\sqrt{2}$ , and the angle of internal reflection is taken as  $\theta=\pi/3$ , which is greater than the critical angle.

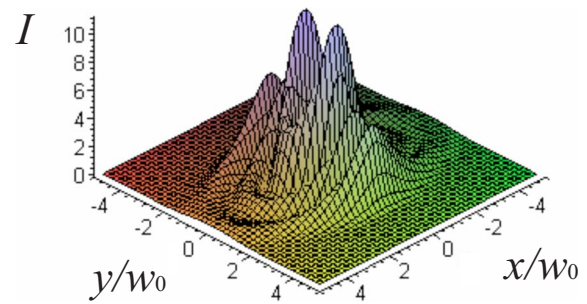
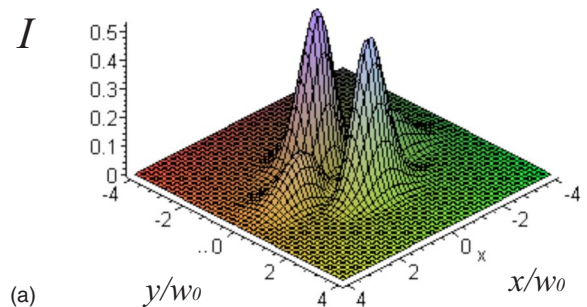


FIG. 4. (Color online) As in Fig. 3, but here the Laguerre-Gaussian beam is such that  $l=3$  and  $p=2$ .

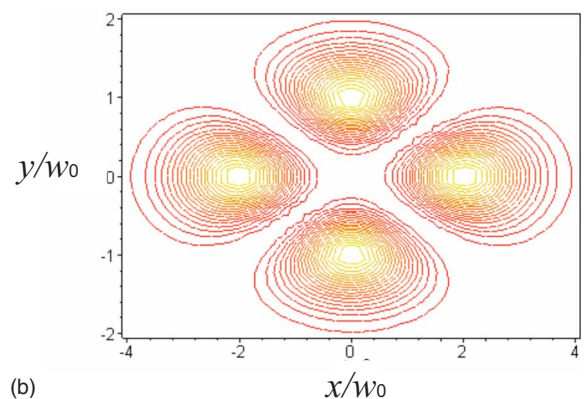
of opposite helicity creating an interference of two surface vortices, in a manner similar to that discussed recently for beams in an unbounded space, where a frequency offset leads to the phenomenon of the optical Ferris wheel [11]. It is easy to see that the total electric field generated in the vacuum region contains the factor

$$\cos\{l \arctan[y/(x \cos \theta)]\}. \quad (9)$$

The appearance of the cosine term in Eq. (9) indicates interference of the two evanescent light beams in the azimuthal direction. Figure 5(a) shows the field distributions for the



(a)



(b)

FIG. 5. (a) (Color online) The intensity distribution (arbitrary units) on the surface at  $z=0$  arising from two copropagating internally reflected Laguerre-Gaussian light beams for which  $l_1=2$ ,  $p_1=0$  and  $l_2=-2$ ,  $p_2=0$ . Distances along the axes are measured in units of the beam waist  $w_0=35\lambda$ , with  $\lambda=590$  nm. (b) The corresponding contour plot. If the beams are slightly different in frequencies such that  $\omega_1 - \omega_2 = \delta$ , the intensity distribution pattern rotates at a frequency  $\delta/2|l_1 - l_2|$ .

case  $l_1=2$ ,  $p_1=0$  and  $l_2=-2$ ,  $p_2=0$ , and the contour plots are shown in Fig. 5(b). If the frequencies of the beams differ slightly, the pattern will rotate at a frequency  $\delta/2|l_1-l_2|$  with  $\delta$  equal to the frequency difference.

In the above analysis, we have outlined the essential physics underlying the phenomenon of surface optical vortices, associated particularly with Laguerre-Gaussian light. We have shown that the intensity distribution for a typical surface optical vortex has a limited spatial extent in the direction normal to the surface in the vacuum region, of the order of a fraction of a wavelength. However, the in-plane distributions mimic those of the incident and internally reflected light and so carry the signature of orbital angular momentum in the incident beam. The optical vortices of a Laguerre-Gaussian basis constitute a complete set for the description of vortices of any desired order defined by the integers  $l$  and  $p$ , so that the phenomenon is quite general. Further work is needed to uncover the properties of surface optical vortices. Useful information can be gained by determining phase profiles, wave-front structures, and energy-momentum flow.

To conclude, we note that in addition to the intrinsic importance of surface optical vortices as physical entities in their own right, some technical applications can be envisaged at this stage. We have briefly mentioned the manipulation of adsorbed atoms and molecules held on surfaces by van der Waal force, and in this connection there has recently been

strong interest in the opportunity for precision manipulation of such atoms. However, it appears that none of the methods suggested so far includes near-resonance optical manipulation along the surface. Optical vortices offer an unprecedented potential for the manipulation of adsorbed atoms congregating in extremum regions of intensity on the surface. The principle can be employed to create patterned surfaces by employing carefully designed sets of incident beams to create a lattice of evanescent light wells. The system also affords the opportunity to manipulate larger objects on the surface, translation and rotation being affected, by moving the spot at which the incident beam strikes the interface. Finally it is to be noted that surface optical vortices of other kinds can be generated from other optical beams carrying orbital angular momentum and that highly significant enhancements of the evanescent light fields can be realized by introducing a metallic film. In the evanescent surface plasmon modes the fields can be at least an order of magnitude larger [18]. Work on surface plasmon optical vortices and guided modes is now in progress, and the results will be reported in due course.

V.E.L. wishes to thank the ESF for financial support under the Programme QUEDDIS Exchange Grant No. 1750, while this work was carried out.

- 
- [1] L. Allen, M. W. Beijersbergen, R. J. C. Spreeuw, and J. P. Woerdman, *Phys. Rev. A* **45**, 8185 (1992).
  - [2] L. Allen, M. J. Padgett, and M. Babiker, in *Progress in Optics XXXIX*, edited by E. Wolf (Elsevier Science B.V., 1999), pp. 291–372.
  - [3] L. Allen, S. M. Barnett, and M. J. Padgett, *Optical Angular Momentum* (Institute of Physics Publishing, Bristol, 2003).
  - [4] *Structured Light and its Applications: An Introduction to Phase-Structured Beams and Nanoscale Optical Forces*, edited by D. L. Andrews (Academic, Burlington, MA, 2008).
  - [5] Special journal issue on optical tweezers [*J. Mod. Opt.* **50**, 1501ff (2003)].
  - [6] M. Babiker, W. L. Power, and L. Allen, *Phys. Rev. Lett.* **73**, 1239 (1994).
  - [7] M. Babiker, C. R. Bennett, D. L. Andrews, and L. C. Dávila Romero, *Phys. Rev. Lett.* **89**, 143601 (2002).
  - [8] D. L. Andrews, A. R. Carter, M. Babiker, and M. Al-Amri, *Proc. SPIE* **6131**, 101 (2006).
  - [9] A. R. Carter, M. Babiker, M. Al-Amri, and D. L. Andrews, *Phys. Rev. A* **72**, 043407 (2005).
  - [10] A. R. Carter, M. Babiker, M. Al-Amri, and D. L. Andrews, *Phys. Rev. A* **73**, 021401(R) (2006).
  - [11] S. Franke-Arnold, J. Leach, M. J. Padgett, V. E. Lembessis, D. Ellinas, A. J. Wright, J. M. Girkin, P. Ohberg, and A. S. Arnold, *Opt. Express* **15**, 8619 (2007).
  - [12] C. R. Bennett, J. B. Kirk, and M. Babiker, *Phys. Rev. A* **63**, 033405 (2001), and references therein.
  - [13] V. Garces-Chavez, K. Dholakia, and G. C. Spalding, *Appl. Phys. Lett.* **86**, 031106 (2005).
  - [14] P. J. Reece, V. Garces-Chavez, and K. Dholakia, *Appl. Phys. Lett.* **88**, 221116 (2006).
  - [15] L. C. Thomson, G. Whyte, M. Mazilu, and J. Courtial, *J. Opt. Soc. Am. B* **25**, 849 (2008).
  - [16] Djenan Ganic, Xiaosong Gan, and Min Gu, *Opt. Express* **12**, 5533 (2004).
  - [17] Baohua Jia, Xiaosong Gan, and Min Gu, *Opt. Express* **16**, 15191 (2008).
  - [18] W. L. Barnes, A. Dereux, and T. W. Ebbesen, *Nature (London)* **424**, 824 (2003).